Nonadiabatic Molecular Dynamics Study of Electron Transfer from Alizarin to the Hydrated Ti^{4+} Ion

Walter R. Duncan and Oleg V. Prezhdo*

Department of Chemistry, University of Washington, Seattle, Washington 98195-1700

Received: May 16, 2005; In Final Form: July 14, 2005

Ab initio real-time nonadiabatic (NA) molecular dynamics (MD) simulations are performed in order to investigate the photoinduced electron transfer (ET) from alizarin to the hydrated Ti^{4+} ion and compare it with the ET into bulk TiO_2 that forms the basis of the Grätzel type solar cell. The experimental data and electronic structure calculations indicate that the photoexcitation spectra of alizarin attached to either bulk TiO_2 or the Ti^{4+} ion in solution are very similar. In contrast, the NAMD simulations at ambient temperature predict marked differences between the ET dynamics that follow the photoexcitation in the two systems. The simulation of ET between alizarin and the TiO_2 surface shows predominantly adiabatic transfer that occurs within 8 fs (Duncan et al. *J. Am. Chem. Soc.* **2005**, *127*, 7941), in agreement with the time-resolved experimental data. The simulation of alizarin attached to the hydrated Ti^{4+} ion reported presently predicts that the ET does occur, but on a slower 30 fs time scale, with a substantially reduced amplitude and by a predominantly NA mechanism. The differences are attributed to the disparity in the acceptor states of bulk TiO_2 and the Ti^{4+} ion in solution. It is shown that the predicted alizarin−Ti^{4+} ET dynamics can be verified experimentally.

I. Introduction

The dye-sensitized nanocrystalline solar cell, also known as the Grätzel cell, is a promising alternative to the more costly traditional solar cell.[1−5] It employs organic or transition-metal-based chromophores that are tuned to visible light and adsorbed to highly porous nanocrystalline titanium dioxide. This inexpensive semiconductor, although it absorbs in the ultraviolet region and is thus not suitable for solar light harvesting on its own, does facilitate the electron−hole separation and conducts free electrons. The cell's electron−hole separation begins with the interfacial electron transfer (ET) from the chromophore to the semiconductor that occurs after the light absorption. The relative yields and rates of electron injection, recombination, and the decay of the chromophore excited state influence the efficiency of the solar cell.[3,6] The competition of charge recombination with the photoinduced ET lowers the photocurrent. The positioning of the photoexcited state energy relative to the bottom edge of the semiconductor conduction band determines the injection efficiency and the magnitude of the voltage loss. While the injection from photoexcited states high above the conduction band edge is most effective, the relaxation of the injected electron to the bottom of the conduction band leads to an experimentally observed photovoltage that is below the theoretical maximum. Improving the photon-to-electron yield and the voltage of solar devices requires a thorough understanding of the competing reaction mechanisms.

Considerable research efforts have been focused on the photoinduced ET dynamics across the chromophore−semiconductor interface.[7−41] The experimental data clearly point to a complex dependence of the ET rates and mechanisms on the chemical and electronic structure of the organic dyes, inorganic semiconductor, and dye−semiconductor binding. Ultrafast laser techniques have shown that electron injection can occur on a femtosecond time scale,[7−22] which is faster than the redistribution of the vibrational energy, and is therefore poorly described by the traditional ET models.[13,42] Two competing mechanisms that require different conditions for optimum performance have been proposed to explain the observed ultrafast ET.[16,17] In the adiabatic mechanism, the coupling between the dye and the semiconductor is large, and ET occurs through a transition state along the reaction coordinate that involves a concerted motion of the nuclei. The electron remains in the same Born−Oppenheimer (adiabatic) state, which changes localization from the dye to the semiconductor along the reaction coordinate. In the nonadiabatic (NA) mechanism, the coupling between the dye and the semiconductor is small, and the ultrafast ET is achieved through multiple direct transitions from the dye state into a manifold of the conduction band acceptor states. The adiabatic transfer can be described by Marcus transition state theory, while the NA ET is typically treated by a perturbation theory, such as the Fermi Golden rule.[42] Intermediate couplings can entail a combination of both ET mechanisms.

The ab initio NA molecular dynamics (MD) simulations of the interfacial ET carried out in our group[35−40] were the first theoretical studies that established the electron injection mechanisms in real time and at the atomistic level of detail. Our studies investigated ET from isonicotinic acid[35−38] and alizarin[38−41] into TiO_2. The alizarin system constitutes a particularly interesting case, since the chromophore photoexcited-state energy is near the bottom of the TiO_2 conduction band. The dynamics of ET from alizarin into TiO_2 are strongly modulated by the fluctuations of the donor and acceptor state energies that are induced by nuclear vibrations. The NAMD simulation reproduced the ultrafast experimental ET time scale and demonstrated that the adiabatic mechanism dominates.[38−40] The adiabatic injection is made possible by a strong alizarin−TiO_2 coupling that leads to efficient electron injection at the edge of the conduction band. The injection scenario that exists in the alizarin−TiO_2 system has the potential to aid in the design

* Corresponding author. E-mail: prezhdo@u.washington.edu.

10.1021/jp052570x CCC: $30.25 © 2005 American Chemical Society
Published on Web 09/01/2005

of cells with higher voltages, since energy is not lost by rapid relaxation to the bottom of the conduction band.[5]

The present study investigates the ET from alizarin to hydrated Ti^{4+} ion, which is the expected form in solution, to the transfer from alizarin to the TiO_2 surface.[38−40] The study is motivated by the fact that the photon absorption that precedes the electron injection is very similar in the two cases. The calculated electronic spectrum of alizarin attached to solvated TiO_2 matches the experimental spectrum of alizarin at the TiO_2 surface.[41] The experimental absorption spectra of the closely related catechol molecule attached to bulk TiO_2 and ligating Ti^{4+} in solution show identical features in the spectral region that is not masked by the bulk TiO_2 absorption.[43] In contrast to alizarin, the photoexcitation of the catechol complexes promotes the electron from the chromophore onto the titanium.[41] The back ET from Ti^{4+} and TiO_2 onto catechol has been studied experimentally.[43] The photoexcitation in the alizarin/titanium systems is localized on the chromophore, allowing one to investigate the forward ET. The periodic density functional theory (DFT) calculations on surface-attached alizarin indicate that the photoexcited state of alizarin has little surface contribution, and that the TiO_2 acceptor state is localized within the first three surface layers.[40] The extended simulation with isonicotinic acid[35−37] predicts an even stronger localization of the acceptor state, with the Ti atom that is bound to the acid contributing over 20%. In view of the strong similarity of the alizarin absorption on the surface and in solution, as well as the notable localization of the surface acceptor state, it is instructive to investigate whether the ET will be similar in the two cases. The NAMD simulations reported below make a prediction regarding the photoinduced dynamics in solution which can be easily tested experimentally.

II. Methods

The molecular structure of alizarin attached to the hydrated Ti^{4+} ion is shown in the top panel of Figure 1. Alizarin is chemically bound to the Ti^{4+} ion through both hydroxyl groups. The bidentate structure gives the most stable binding between the alizarin and the TiO_2 surface, as follows from the ab initio molecular orbital and DFT studies by Thurnauer *at el.* on the related catechol molecule.[44] The bidentate binding of alizarin to the hydrated Ti^{4+} ion is also more favorable than monodentate binding. The remaining four sites of Ti^{4+} are occupied by a set of water and hydroxyl ligands, as expected for a neutral complex in solution. The NAMD simulation of alizarin bound to a single titanium is performed with the methodology developed previously for periodic systems.[35−40] Sufficient vacuum is added around the entire structure, giving a cell with the dimensions $13 \times 15 \times 21$ Å^3.

The electronic structure and spectrum of alizarin bound to Ti^{4+} are investigated using linear-response TDDFT with the B3LYP[45,46] and the PW91[47] exchange-correlation functionals. The calculations summarized in Table 1 are performed with the Gaussian 98 software using the 6-31g** basis.[48] The electron injection dynamics are investigated with NAMD TDDFT using the VASP code,[49−51] the PW91 exchange-correlation functional,[47] the Vanderbilt pseudopotentials[52] and a numerically converged plane wave basis. The NAMD functionality is added[35−40] to the standard VASP code distribution.

The time dependence in the NAMD TDDFT simulations originates from the atomic motions that induce NA transitions between the electronic states. The simulation procedure is detailed in refs 35 and 40. Briefly: following geometry optimization, the system is brought to equilibrium at ambient temperature by MD with repeated velocity rescaling. A 1000 fs ground-state adiabatic MD is then run in the microcanonical ensemble with a 1 fs time step. Initial conditions for NAMD are sampled along the ground-state trajectory. Under the classical path approximation,[53] this trajectory is used to compute the NA dynamics.

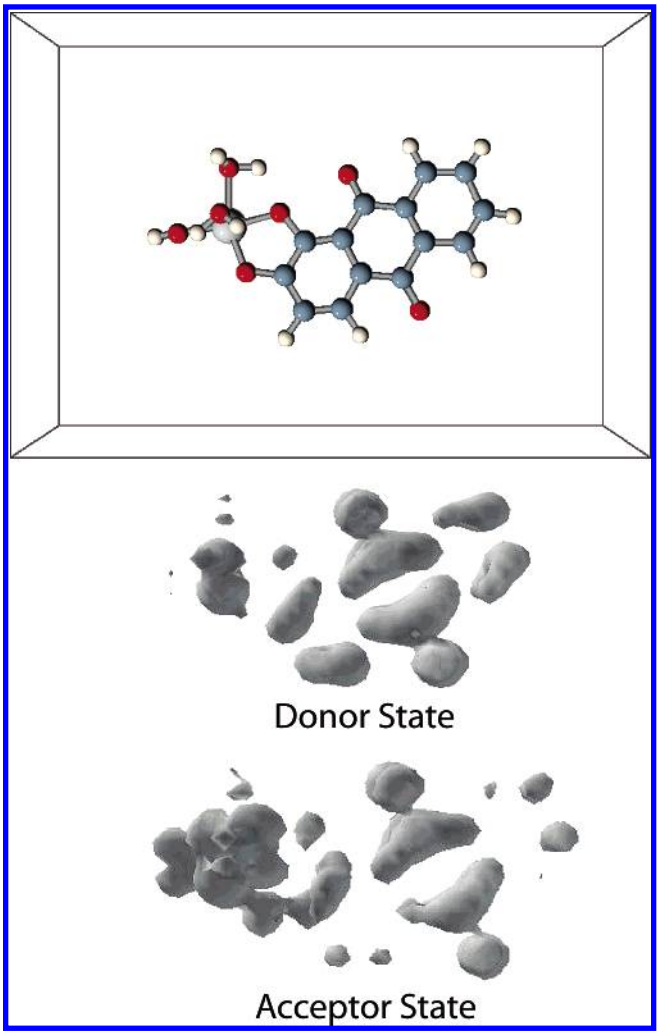

Figure 1. Molecular structure and densities of electron donor and acceptor states for alizarin attached to the hydrated Ti^{4+} ion.

TABLE 1: Energies (E), Wavelengths (λ), Oscillator Strengths (osc), and Transition Dipole Moments (d_X, d_Y, d_Z) of the Five Lowest Electronic Transitions of Alizarin Attached to the Hydrated Ti^{4+} Ion[a]

state	E (eV)	λ (nm)	osc (au)	d_X (au)	d_Y (au)	d_Z (au)
			B3LYP			
1	2.94	422	0.0013	−0.0140	−0.0187	−0.1319
2	3.02	411	0.1012	−0.0535	−0.1530	−1.1585
3	3.17	391	0.0444	−0.0026	0.1094	−0.7478
4	3.33	372	0.0002	0.0028	0.0026	0.0457
5	3.44	361	0.0015	−0.0082	−0.1244	0.0411
			PW91			
1	2.32	534	0.0003	−0.0097	−0.0135	−0.0763
2	2.49	497	0.0732	−0.0401	−0.1162	−1.0879
3	2.61	476	0.0115	−0.0172	0.0131	−0.4246
4	2.70	460	0.0060	0.0002	−0.0510	0.2979
5	2.71	458	0.0070	0.0120	0.1292	−0.2974

[a] The calculations were performed with linear-response time-dependent density functional theory using the B3LYP and PW91 functionals and the 6-31g** Gaussian basis.[48] The experimental maximum is at 500 nm.[22]

The charge density $\rho(\mathbf{r}, t)$ within the Kohn−Sham DFT[54] is expressed by a sum over the Kohn−Sham orbitals $\psi_n(\mathbf{r}, t)$ occupied by N_e electrons

$$\rho(\mathbf{r}, t) = \sum_{n=1}^{N_e} |\psi_n(\mathbf{r}, t)|^2 \quad (1)$$

The TD variational principle leads to the following set of equations for the evolution of the Kohn−Sham orbitals[55,56]

$$i\hbar \frac{\partial}{\partial t}\psi_n(\mathbf{r}, t) = H(\mathbf{r}, \mathbf{R}(t))\psi_n(\mathbf{r}, t), \quad n = 1, 2, ..., N_e \quad (2)$$

where $H(\mathbf{r}, \mathbf{R}(t))$ depends on time through the atomic motions $\mathbf{R}(t)$. These one-electron TD Kohn−Sham equations are coupled through the dependence of the DFT functional H on the total electron density (eq 1).

The TD one-electron wave functions $\psi_n(\mathbf{r}, t)$ are expanded in the basis of adiabatic Kohn−Sham orbitals $\phi_k(\mathbf{r}, \mathbf{R}(t))$

$$\psi_n(\mathbf{r}, t) = \sum_k c_{nk}(t)\phi_k(\mathbf{r}, \mathbf{R}(t)) \quad (3)$$

that are obtained by a time-independent DFT calculation for the current atomic positions. Inserting the expansion into the TD Kohn−Sham equation (eq 2) gives the evolution for the coefficients

$$i\hbar \frac{\partial}{\partial t}c_j(t) = \sum_k c_k(t)(\epsilon_k \delta_{jk} + d_{jk}) \quad (4)$$

where ϵ_k is the energy of the adiabatic orbital k and $d_{jk} = -i\hbar \langle\phi_j|\nabla_{\mathbf{R}}|\phi_k\rangle \cdot d\mathbf{R}/dt$ is the NA coupling between orbitals j and k. The NA coupling is calculated numerically by the overlap of orbitals j and k at sequential time steps.[57] The propagation of eq 2 is performed by the second order differencing scheme[58] with a 10^{-3} fs time step.

The configuration interaction singles (CIS) and linear-response TDDFT calculations[41] indicate that the photoexcitation in the systems under investigation is well described by an electronic transition from the highest occupied molecular orbital (HOMO) to a virtual orbital that best matches the lowest unoccupied orbital (LUMO) of free alizarin. The ET dynamics are determined by the evolution (2) of the photoexcited virtual orbital. The ET progress is monitored by calculating the photoexcited-state electron density that has left the region of the simulation cell occupied by the dye. The changes in the photoexcited-state electron density occur by changes in either adiabatic Kohn−Sham orbital ϕ_k localizations or expansion coefficient c_{nk}, cf. eq 3. These two contributions to the ET dynamics are responsible for the adiabatic and NA ET mechanisms, respectively.[35−40]

III. Results and Discussion

The densities of the donor and acceptor states for alizarin attached to the hydrated Ti^{4+} ion are shown in the middle and bottom panels of Figure 1, respectively. The donor state of the Ti^{4+} system is very similar to that of the bulk-TiO_2 system, cf. Figure 5 of ref 40, in agreement with the experimental photoexcitation spectra[21,43] and the ab initio electronic structure calculations.[41] Following the photoexcitation from the ground state into the donor state, the electron is transferred nonradiatively into the acceptor state. The densities of the acceptor states are markedly different in the two systems, cf. the botton panels of Figure 1 in the present paper and Figure 5 of ref 40, suggesting that the ET dynamics on the surface and in solution should show different signatures.

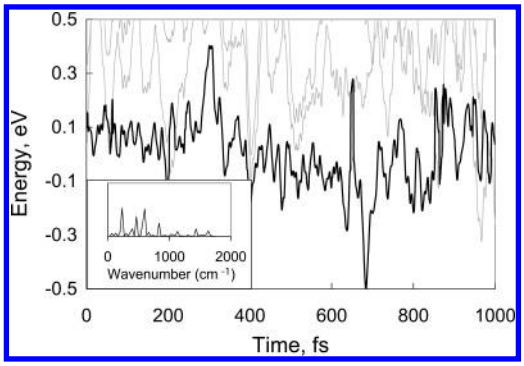

Figure 2. Evolution of the excited-state energies, with the photoexcited-state marked by the bold line, for alizarin attached to the hydrated Ti^{4+} ion. Inset: Fourier transforms of the photoexcited-state energy.

The alizarin/bulk-TiO_2 donor is a π-electron state that is spread over all three rings of the chromophore, Figure 5 of ref 40. A distribution of ionic coordinates creates an inhomogeneous broadening of the alizarin/bulk-TiO_2 spectrum and an ensemble of photoexcited states. Usually, the photoexcited state is slightly below the edge of the TiO_2 conduction band, and only a small amount of the electron density extends onto the surface Ti atom to which the dye is attached. In the cases where the photoexcited state is inside the conduction band, partial ET can take place already during the photoexcitation, and the photoexcited-state becomes delocalized into the bulk. On average, about 70% of the photoexcited-state density in the alizarin/bulk-TiO_2 system is localized on alizarin. The donor state for the Ti^{4+} system is shown in the middle panel of Figure 1. On average, 85% of the photoexcited state in the alizarin/Ti^{4+} system is localized on alizarin. This percentage is higher for the single Ti case than for bulk-TiO_2, since there is no conduction band to interact with.

While the correspondence between the donor states of the surface and solution systems is responsible for the similarity of the corresponding absorption spectra,[21,41,43] the differences in the ET dynamics are mainly due to the contrast between the acceptor states, cf. bottom panels in Figure 1 in the present paper and Figure 5 of ref 40. The alizarin/bulk-TiO_2 acceptor state is composed of Ti d-orbitals and spreads out roughly radially from the attachment point, with almost no density beyond the third Ti layer. The d-orbitals in the adjacent layers are perpendicular to each other in a configuration that maximizes their overlap. Without a semiconductor slab to delocalize into, the acceptor state for the single titanium system represents only a moderate shift of the electron density from the chromophore onto the Ti and surrounding ligands. Therefore, substantially less ET is expected in the smaller system.

It should be noted that states similar to the acceptor state for the Ti^{4+} system, Figure 1, do exist in the surface system. However, they are buried in the multitude of the surface and bulk states, and contribute little to the ET dynamics. Although one could have expected that the photoexcited dynamics involving bulk-TiO_2 proceed first to the acceptor state seen in solution, Figure 1, and only later to the bulk acceptor states, it is not the case. The photoexcited electron moves directly from alizarin into the bulk.

The ET dynamics are dictated by both the spatial localization of the donor and acceptor states and their relative positioning in energy. Figure 2 shows the energies of the photoexcited state (bold line) and Ti^{4+} states (thin gray lines) for the 1000 fs run. The zero of energy corresponds to the average energy of the photoexcited state. Compared to bulk-TiO_2, Figure 6a of ref

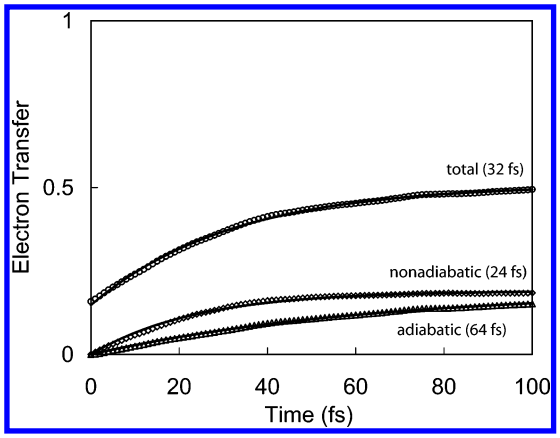

Figure 3. ET dynamics from alizarin to the hydrated Ti^{4+} ion. Shown are the total ET as well as its adiabatic and NA contributions. The thick black lines are exponential fits, eq 5, with the time scales shown on the figure.

40, far fewer acceptor states are available in solution, and the photoexcited state is the system LUMO 90% of the time. The alizarin/bulk-TiO_2 photoexcited state energy has a standard deviation of approximately 0.15 eV. This is small when compared to the TiO_2 band gap of 3.5 eV,[43] or the alizarin excitation energy of 2.5 eV,[21] but it is large enough to move the photoexcited state in to and out of the conduction band. The energy oscillates with frequencies at and below 700 cm^{-1} due to bending and torsional nuclear motions. The standard deviation of the photoexcited-state energy in solution is 0.13 eV, which is very similar to the one seen with bulk-TiO_2, supporting the fact that the photoexcited state of the bulk system does not extend beyond the first Ti atom of the surface. Compared to the bulk-TiO_2 case, the Fourier transform of the photoexcited energy in the alizarin/Ti^{4+} system shows almost the same frequencies, but with substantially different amplitudes, cf. Figure 7a of ref 40 and the insert of Figure 2 in the present paper. Stronger contributions from the higher frequency vibrations are seen with the smaller system, as should be expected. The more prominent low-frequency features in the Fourier transform of the photoexcited-state energy of the extended system indicate that alizarin participates in normal mode vibrations that involve multiple surface atoms.

The ET dynamics are shown in Figure 3. The total ET (circles), the adiabatic ET (triangles), and the NA ET (diamonds) are averages over 900 NAMD runs. The total ET is fit with the exponential equation (thick black line)

$$\mathrm{ET}(t) = \mathrm{ET}_f(1 - \exp[-(t + t_0)/\tau]) \qquad (5)$$

where ET_f is the final amount of ET, and τ is the ET time scale. The t_0 term reflects the initial delocalization of the photoexcited state on the Ti, and it can be interpreted as the amount of time that the photoexcitation advances the ET along the reaction coordinate. The same equation, with $t_0 = 0$, calculates the fits to the adiabatic and NA ET.

In the alizarin/bulk-TiO_2 system the electron is on average 30% delocalized onto the semiconductor after the photoexcitation. The ET continues nonradiatively with a time constant of 7.9 fs, Figure 10a of ref 40. The adiabatic mechanism controls the dynamics and is not only faster, but also reaches a much higher value than the NA component. The adiabatic transfer is very efficient in this case, because alizarin is directly bound to bulk-TiO_2, creating a strong interaction between alizarin's conjugated π-electron system and the TiO_2 conduction band, which is composed of the Ti d-orbitals. A number of surface acceptor states exist and are given the opportunity to cross energetically with the alizarin donor state. The vibrationally induced crossings of the energies of the strongly coupled donor and acceptor produce transitions states for the adiabatic transfer. Quantum jumps that are responsible for the NA transfer take place on a slower time scale in the alizarin/bulk-TiO_2 system.[40]

The ET dynamics of the system that consist of alizarin attached to a titanium in solution, Figure 3, are different in several key ways, all of which can be traced to the nature of the donor and acceptor states, and the lower number of acceptor states. 85% of the photoexcited state in solution is, on average, localized on the chromophore, compared to 70% in the surface system. The acceptor state in solution has a large amount of electron density spread onto the chromophore, Figure 1. ET into this state leaves nearly 50% of the electron on the dye. The transfer occurs on the 32 fs time scale, 4 times slower than that for bulk-TiO_2. The significantly smaller number of acceptor states seen with the hydrated Ti^{4+} ion create infrequent donor−acceptor crossings. There are five d-orbitals in the Ti atom that can potentially accept the photoexcited electron; only the lowest two d-orbitals cross with the π-state of alizarin, Figure 2. The adiabatic transfer rate is dramatically slowed from 7.1 fs with bulk-TiO_2 to 64 fs in solution. The NA ET is also slower, since the NA acceptor states are few and farther in energy from the photoexcited state. However, the difference in NA ET time scales is only a factor of 2, compared to the factor of 9 for the adiabatic ET. The NA mechanism is more efficient than the adiabatic mechanism and, therefore, dictates the overall ET in the Ti^{4+} system.

The question remains, can the electron injection dynamics in the alizarin/Ti^{4+} system be detected experimentally? The photoexcited electron in the surface system leaves the chromophore altogether and can be detected either directly in the TiO_2 conduction band[15−20] or by spectroscopy of the chromophore cation.[9−14,21,22] The electron never entirely disappears from alizarin in the hydrated Ti^{4+} system. Still, the photoexcited electron dynamics can be detected as evidenced by the calculated transition dipole moments and oscillator strengths of the five lowest states, Table 1. The difference between the oscillator strength of the photoexcited donor state and the oscillator strengths of the acceptor states is substantial and can be detected with stimulated emission. All transition dipole moments are polarized from alizarin to titanium, rendering polarization measurements ineffective. It can be expected that further excitation of either donor or acceptor states can be used to monitor the electron injection dynamics as well.

IV. Conclusions

The NAMD simulations showed major variations in the photoinduced ET from alizarin to the hydrated Ti^{4+} compared with the TiO_2 surface. The solution dynamics are 4 times slower, have a factor of 2 smaller amplitude, and proceed by a predominantly NA mechanism. In contrast, the electron injection into bulk-TiO_2 is ultrafast, results in a complete removal of the electron density from the chromophore, and occurs adiabatically.[40] The differences in the ET dynamics arise from the disparity in the density of the acceptor states of the bulk and the solution systems. The electronic structure analysis indicates that the simulated photoexcitation dynamics in the alizarin/Ti^{4+} system can be verified spectroscopically.

Acknowledgment. The research was supported by NSF, CAREER Award CHE-0094012 and PRF, Award 150393. O.V.P. is an Alfred P. Sloan Fellow and is grateful to Dr. Jan

Michael Rost at the Max Planck Institute for the Physics of Complex Systems, Dresden, Germany, for his hospitality during manuscript preparation.

References and Notes

(1) O'Regan, B.; Grätzel, M. *Nature (London)* **1991**, *353*, 737.
(2) Schwarz, O.; van Loyen, D.; Jockusch, S.; Turro, N. J.; Duerr, H. *J. Photochem. Photobiol. A: Chem.* **2000**, *132*, 91.
(3) McConnell, R. D. *Renew. Sustain. Energy Rev.* **2002**, *6*, 273.
(4) Nozik, A. J. *Physica, E.* **2002**, *14*, 115.
(5) Grätzel, M. *J. Photochem. Photobiol. C: Photochem. Rev.* **2003**, *4*, 145.
(6) Huang, S. Y.; Schlichthorl, G.; Nozik, A. J.; Gratzel, M.; Frank, A. J. *J. Phys. Chem. B* **1997**, *101*, 2576.
(7) Tachibana, Y.; Moser, J. E.; Grätzel, M.; Klug, D. R.; Durrant, J. R. *J. Phys. Chem. B* **1996**, *100*, 20056.
(8) Ravirajan, P.; Haque, S. A.; Poplavskyy, D.; Durrant, J. R.; Bradley, D. D. C.; Nelson, J. *Thin Solid Films* **2004**, *451*−*452*, 624.
(9) Burfeindt, B.; Hannappel, T.; Storck, W.; Willig, F. *J. Phys. Chem. B* **1996**, *100*, 16463.
(10) Hannappel, T.; Burfeindt, B.; Storck, W.; Willig, F. *J. Phys. Chem. B* **1997**, *101*, 6799.
(11) Ramakrishna, S.; Willig, F. *J. Phys. Chem. B* **2000**, *104*, 68.
(12) Ramakrishna, S.; Willig, F.; May, V.; Knorr, A. *J. Phys. Chem. B* **2003**, *107*, 607.
(13) Schwarzburg, K.; Erntorfer, R.; Felber, S.; Willig, F. *Coord. Chem. Rev.* **2004**, *248*, 1259.
(14) Gundlach, L.; Felber, S.; Storck, W.; Galoppini, E.; Wei, Q.; Willig, F. *Res. Chem. Intermed.* **2005**, *31*, 39.
(15) Ellingson, R. J.; Asbury, J. B.; Ferrere, S.; Ghosh, H. N.; Sprague, J. R.; Lian, T.; Nozik, A. J. *J. Phys. Chem. B* **1998**, *102*, 6455.
(16) Asbury, J. B.; Ellingson, R. J.; Ghosh, H. N.; Nozik, A. J.; Ferrere, S.; Lian, T. *J. Phys. Chem. B* **1999**, *103*, 3110.
(17) Asbury, J. B.; Hao, E. C.; Wang, Y. Q.; Ghosh, H. N.; Lian, T. Q. *J. Phys. Chem. B* **2001**, *105*, 4545.
(18) Anderson, N. A.; Hao, E.; Ai, X.; Hastings, G.; Lian, T. *Physica E* **2002**, *14*, 215.
(19) Asbury, J. B.; Anderson, N. A.; Hao, E. C.; Ai, X.; Lian, T. Q. *J. Phys. Chem. B* **2003**, *107*, 7376.
(20) Ai, X.; Anderson, N. A.; Guo, J. C.; Lian, T. Q. *J. Phys. Chem. B* **2005**, *109*, 7088.
(21) Huber, R.; Spoerlein, S.; Moser, J. E.; Grätzel, M.; Wachtveitl, J. *J. Phys. Chem. B* **2000**, *104*, 8995.
(22) Huber, R.; Moser, J. E.; Grätzel, M.; Wachtveitl, J. *J. Phys. Chem. B* **2002**, *106*, 6494.
(23) Derosa, P. A.; Seminario, J. M. *J. Phys. Chem. B* **2001**, *105*, 471.
(24) Fan, F. F.; Yao, Y.; Cai, L.; Cheng, L.; Tour, J. M.; Bard, A. J. *J. Am. Chem. Soc.* **2004**, *126*, 4035.
(25) Yasutomi, S.; Morita, T.; Imanishi, Y.; Kimura, S. *Science* **2004**, *304*, 1944.
(26) Zhao, W.; Ma, W. H.; Chen, C. C.; Zhao, J. C.; Shuai, Z. G. *J. Am. Chem. Soc.* **2004**, *126*, 4782.
(27) Hirakawa, T.; Whitesell, J. K.; Fox, M. A. *J. Phys. Chem. B* **2004**, *108*, 10213.
(28) Cozzoli, P. D.; Fanizza, E.; Comparelli, R.; Curri, M. L.; Agostiana, A.; Laub, D. *J. Phys. Chem. B* **2004**, *108*, 9623.
(29) Ho, W.; Yu, J. C.; Lin, J.; Yu, J.; Li, P. *Langmuir* **2004**, *20*, 5865.
(30) Kim, H. G.; Hwang, D. W.; Lee, J. S. *J. Am. Chem. Soc.* **2004**, *126*, 8912.
(31) Zhu, X. Y. *J. Phys. Chem. B* **2004**, *108*, 8778.
(32) Thoss, M.; Kondov, I.; Wang, H. *Chem. Phys.* **2004**, *304*, 169.
(33) Rego, L. G. C.; Batista, V. S. *J. Am. Chem. Soc.* **2003**, *125*, 7989.
(34) Rego, L. G. C.; Abuabara, S. G.; Batista, V. S. *J. Chem. Phys.* **2005**, *122*, 154709.
(35) Stier, W.; Prezhdo, O. V. *J. Phys. Chem. B* **2002**, *106*, 8047.
(36) Stier, W.; Prezhdo, O. V. *J. Mol. Struct. (THEOCHEM)* **2002**, *630*, 33.
(37) Stier, W.; Prezhdo, O. V. *Isr. J. Chem.* **2002**, *42*, 213.
(38) Stier, W.; Duncan, W. R.; Prezhdo, O. V. *SPIE Proc.* **2003**, *5223*, 132.
(39) Stier, W.; Duncan, W. R.; Prezhdo, O. V. *Adv. Mater.* **2004**, *16*, 240.
(40) Duncan, W. R.; Stier, W. M.; Prezhdo, O. V. *J. Am. Chem. Soc.* **2005**, *127*, 7941.
(41) Duncan, W. R.; Prezhdo, O. V. *J. Phys. Chem. B* **2005**, *109*, 365.
(42) Memming, R. *Semiconductor Electrochemistry;* Wiley-VCH: Weinheim, Germany, 2001.
(43) Wang, Y.; Hang, K.; Anderson, N. A.; Lian, T. *J. Phys. Chem. B* **2003**, *107*, 9434.
(44) Redfern, P. C.; Zapol, P.; Curtiss, L. A.; Rajh, T.; Thurnauer, M. C. *J. Phys. Chem. B* **2003**, *107*, 11419.
(45) Becke, A. D. *J. Chem. Phys.* **1993**, *98*, 5648.
(46) Lee, C.; Yang, W.; Parr, R. G. *Phys. Rev. B* **1988**, *37*, 785.
(47) Perdew, J. P. *Electronic Structure of Solids*; Akademie Verlag: Berlin, 1991.
(48) Frisch, M. J.; Trucks, G. W.; Schlegel, H. B.; Scuseria, G. E.; Robb, M. A.; Cheeseman, J. R.; Zakrzewski, V. G.; Montgomery, J. A.; Stratmann, R. E.; Burant, J. C.; Dapprich, S.; Millam, J. M.; Daniels, A. D.; Kudin, K. N.; Strain, M. C.; Farkas, O.; Tomasi, J.; Barone, V.; Cossi, M.; Cammi, R.; Mennucci, B.; Pomelli, C.; Adamo, C.; Clifford, S.; Ochterski, J.; Petersson, G. A.; Ayala, P. Y.; Cui, Q.; Morokuma, K.; Malick, D. K.; Rabuck, A. D.; Raghavachari, K.; Foresman, J. B.; Cioslowski, J.; Ortiz, J. V.; Stefanov, B. B.; Liu, G.; Liashenko, A.; Piskorz, P.; Komaromi, I.; Gomperts, R.; Martin, R. L.; Fox, D. J.; Keith, T.; Al-Laham, M. A.; Peng, C. Y.; Nanayakkara, A.; Gonzalez, C.; Challacombe, M.; Gill, P. M. W.; Johnson, B.; Chen, W.; Wong, M. W.; Andres, J. L.; Gonzalez, C.; Head-Gordon, M.; Replogle, E. S.; Pople, J. A. *Gaussian 98*; Gaussian, Inc.: Pittsburgh, PA, 1998.
(49) Kresse, G.; Hafner, J. *Phys. Rev. B* **1994**, *49*, 14251.
(50) Kresse, G.; Furthmüller, J. *Comput. Mater. Sci.* **1996**, *6*, 15.
(51) Kresse, G.; Furthmüller, J. *Phys. Rev. B* **1996**, *54*, 11169.
(52) Vanderbilt, D. *Phys. Rev. B* **1990**, *41*, 7892.
(53) Berne, B. J.; Ciccotti, G.; Coker, D. F., Eds. *Classical and Quantum Dynamics in Condensed Phase Simulations;* World Scientific: Singapore, 1998.
(54) Kohn, W.; Sham, L. J. *Phys. Rev.* **1965**, *140*, 1133.
(55) Frauenhelm, T.; Seifert, G.; Elstner, M.; Niehaus, T.; Kohler, C.; Amkreutz, M.; Sternberg, M.; Hajnal, Z.; DiCarlo, A.; Suhai, S. *J. Phys.: Condens. Matter* **2002**, *14*, 3015.
(56) Marques, M. A. L.; Gross, E. K. U. *Annu. Rev. Phys. Chem.* **2004**, *55*, 427.
(57) Hammes-Schiffer, S.; Tully, J. C. *J. Chem. Phys.* **1994**, *101*, 4657.
(58) Leforestier, C.; Bisseling, R. H.; Cerjan, C.; Feit, M. D.; Friesner, R.; Guldberg, A.; Hammerich, A.; Jolicard, G.; Karrlein, W.; Meyer, H. D.; Lipkin, N.; Roncero, O.; Kosloff, R. *J. Comput. Phys.* **1991**, *94*, 59.